Tuning the orbital moment in transition metal compounds using ligand states

2001 J. Phys.: Condens. Matter 13 4553

(http://iopscience.iop.org/0953-8984/13/20/316)

INSTITUTE OF PHYSICS PUBLISHING JOURNAL OF PHYSICS: CONDENSED MATTER

J. Phys.: Condens. Matter **13** (2001) 4553–4566 www.iop.org/Journals/cm PII: S0953-8984(01)21600-2

Tuning the orbital moment in transition metal compounds using ligand states

I Galanakis[1,2,5], M Alouani[1], P M Oppeneer[3], H Dreyssé[1] and O Eriksson[4]

[1] Institut de Physique et Chimie des Matériaux de Strasbourg, UMR 7504 CNRS-ULP, F-67037, Strasbourg, France
[2] Institut für Festkörperforschung, Forschungszentrum Jülich, D-52425 Jülich, Germany
[3] Institute of Solid State and Materials Research, PO Box 270016, D-01171 Dresden, Germany
[4] Department of Physics, Uppsala University, Box 530, S-75112 Uppsala, Sweden

E-mail: i.galanakis@fz-juelich.de

Received 1 February 2001, in final form 9 April 2001

Abstract

The influence of ligand states on the orbital magnetism of a 3d atom in a ferromagnetic compound has been studied using an *ab initio* technique. It is shown, using VAu_4, $MnAu_4$ and VPt_3 as examples, that the large spin–orbit coupling of the 5d atom is responsible for the reversal of the coupling between the V(Mn) spin and orbital moments with respect to that for similar compounds. The VAu_4 compound has a large magneto-crystalline anisotropy (MCA) and the spin-up states are completely occupied, which makes its MCA proportional to the orbital moment anisotropy as stated by Bruno's perturbative formula (Bruno P 1989 *Phys. Rev.* B **39** 865). For the latter compound it is also shown that a partial substitution of copper for gold decreases the vanadium orbital moment and hence the MCA. The ligand state effects on the orbital moment together with this alloying procedure may initiate a new approach in the search for ultra-soft magnetic materials.

1. Introduction

Binary alloys consisting of a paramagnet and a ferromagnet have attracted considerable attention over recent years, principally due to their potential utilization in industrial applications. Materials with 1:1 stoichiometry like FePt, FePd and CoPt have been especially thoroughly studied, as their growth is easily controlled using modern techniques like molecular beam epitaxy (MBE) due to the existence of a preferred growth axis for which the structure can be seen as alternating layers of pure atomic species. Other binary compounds have also attracted much attention, like the XPt_3 and XAu_4 family compounds. Two of the most interesting materials are VAu_4 and VPt_3 which are two of the rare cases of a ferromagnet consisting of two materials that in their bulk form are paramagnets. Obviously, the influence of the

[5] Author to whom any correspondence should be addressed.

0953-8984/01/204553+14$30.00

hybridization between the d orbitals of vanadium and Au(Pt) governs the magnetic properties of such a material. The other members of the XAu_4 family present diverse characters: $TiAu_4$ is a paramagnet, $MnAu_4$ is a strong ferromagnet and finally $CrAu_4$ is an antiferromagnet [1]. As for the XPt_3 family, $TiPt_3$ is paramagnet, $MnPt_3$ is a strong ferromagnet while $CrPt_3$ is a ferrimagnet [2].

Several experiments have been carried out for the VAu_4 compound and most of them concern single crystals. Creveling *et al* were the first to discover the ferromagnetic character of VAu_4 [3]. The ordered sample was prepared taking advantage of the order–disorder transition that this material undergoes. Creveling *et al* showed that the susceptibility follows a Curie–Weiss law with a Curie temperature of 60 K [4]. They also measured a vanadium spin magnetic moment of 0.5 μ_B. Adachi *et al* showed that the crystal was characterized by a twin structure and predicted an extraordinary magneto-crystalline anisotropy (MCA) [5]. They also showed that the shape anisotropy, due to the magnetic dipole interactions, is two orders of magnitude smaller than the MCA. Finally, by means of Mössbauer measurements they found a Curie temperature of 61 K and that the spin magnetic moment on the vanadium atoms is 1 μ_B, equal to the effective moment in the paramagnetic state and larger than the value obtained by Creveling *et al*. Kido *et al* verified the value obtained by Adachi *et al* for the vanadium spin magnetic moment using a saturating magnetic field of 350 kOe [6]. This large saturation field is due to the creation of magnetic domains as the material undergoes the order–disorder transition. Chin *et al* showed that any one of the three a-axes of the disordered fcc phase can become the c-axis of the ordered bct structure leading to an orthogonal arrangement of the three domains and hence to a huge saturation field [7]. This explained the small vanadium spin magnetic moments found by other experiments. Sill *et al* studied the effect of the partial substitution of iron for vanadium and found that for a concentration of up to 7% of iron the effective spin moment and the Curie temperature were increased, but at a concentration of 9% of iron the loss of chemical ordering led to a considerable reduction of both the effective spin moment and the Curie temperature [8]. Finally, Claus *et al* showed that the disordered phase is non-magnetic [9]. For $MnAu_4$ the spin magnetic moment has been measured by Yessik *et al* [10].

Kübler was the first to study the VAu_4 compound using the non-relativistic augmented-spherical-wave (ASW) method and obtained a large spin magnetic moment at the vanadium site [11]. Oppeneer *et al* [12] using the relativistic ASW found also a large vanadium total magnetic moment of 1.90 μ_B and a huge Kerr effect anisotropy that appears to be correlated with the orbital moment anisotropy. Oppeneer *et al* also studied $MnAu_4$ and found a total manganese magnetic moment of 4.02 μ_B [12]. Finally Yahagi *et al* [1] used a tight-binding model to calculate the MCA of VAu_4 by means of a Raubenheimer and Gilat method and found that the easy-magnetization axis is the c-axis in agreement with the experiment of Adachi *et al* [5].

The entire V–Pt system is known to be paramagnetic with the exception of VPt_3 which is ferromagnetic [13], with a Curie temperature much larger than that of the VAu_4 compound (T_C = 210–240 K) [14]. Jesser *et al* showed that the VPt_3 compound can crystallize in two structures [14], the metastable $AuCu_3$ structure and the $TiAl_3$ ground-state structure. Kawakami and Goto performed NMR experiments for VPt_3 in the $AuCu_3$ structure and estimated the spin magnetic moments [15]. Several calculations have been performed for this compound especially in the $AuCu_3$ structure [2, 11, 16–18], where vanadium has a spin magnetic moment comparable to that in VAu_4. The $TiAl_3$ structure was studied by Kübler [11] and by Auluck and Nautiyal [18] who included also the spin–orbit coupling in their calculations.

In this contribution we use the relativistic full-potential version of the linear muffin-tin orbital (FP-LMTO) method [19] in conjunction with the local spin-density approximation

(LSDA) [20, 21] to study the magnetic properties of the three compounds VAu_4, $MnAu_4$ and VPt_3. In sections 3 and 4 we present the calculated MCA and magnetic moments. Our calculated spin quantization axis is in agreement with experiments for VAu_4 [5]. Orbital moments show a large anisotropy for the vanadium and the manganese atoms, that is explained in terms of the m_ℓ-projected d density of states (DOS). In section 5 we discuss the violation of the third Hund's rule by the vanadium atoms in both VAu_4 and VPt_3 for the relative direction of the spin and orbital magnetic moments. We show that this phenomenon originates from the influence of the large spin–orbit coupling of the gold and platinum atoms on the magnetic properties of the vanadium atom. This last feature leads us to propose a new way to build ultra-soft magnetic materials (using $V(Au_xCu_{1-x})_4$ as an example) that can be used in various applications like AC converters where one minimizes the MCA.

2. Computation details

The VAu_4 and $MnAu_4$ compounds crystallize in the Ni_4Mo ($D1_a$) phase. This structure is characterized by a bct Bravais lattice with vanadium or manganese atoms at the bct lattice positions and four gold atoms around each transition metal atom, as can be seen in figure 1, where we have projected on the (001) plane two successive layers corresponding to $z = 0$ (circles) and $z = c/2$ (diamonds). In our calculations we used the experimental lattice parameters, which are: $a = 6.382$ Å and $c/a = 0.624$ for VAu_4 and $a = 6.45$ Å and $c/a = 0.625$ for $MnAu_4$. The c/a ratios are close to the ideal value $\sqrt{2/5} \simeq 0.632$ for which each transition metal atom has twelve equidistant gold atoms as nearest neighbours. Notice that among the next-nearest 3d transition metal neighbours only two are also of the same type, i.e. the vanadium atoms are arranged in chains parallel to the c-axis. The unit cell contains one transition metal atom with coordinates $(0, 0, 0)$—the x-axis is along the [100] direction and the y-axis along the [010]—and four gold atoms at the positions $(x, y, 0)$, $(-x, -y, 0)$, $(-y, x, 0)$ and $(y, -x, 0)$, where $x = 0.2a$ and $y = 0.4a$.

The VPt_3 compound crystallizes either in the metastable $AuCu_3$ structure ($L1_2$) or in the $TiAl_3$ structure (DO_{22}) which is the ground state. Its lattice parameters are $a = 3.861$ Å

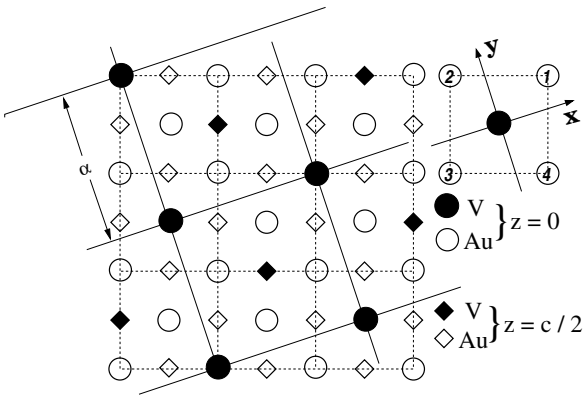

Figure 1. A schematic view of the Ni_4Mo structure adopted by the XAu_4 compounds. The transition metal atoms occupy the positions of a bct structure with four gold atoms surrounding each one of them. With circles we represent the atoms at the $z = 0$ layer and with diamonds the $z = c/2$ layer. The c/a ratio is very close to the ideal $\sqrt{2/5}$ for both VAu_4 and $MnAu_4$. Each transition metal atom has 12 gold atoms as first neighbours. Notice that among the next-nearest neighbours only two are transition metal atoms.

and $c/a = 2.027$ for the tetragonal $TiAl_3$ structure [22], and $a = 3.87$ Å for VPt_3 in the cubic $AuCu_3$ structure [14] (see figure 2). The two structures have the same type of nearest neighbour, so their relative stability is determined by the next-nearest- and further-neighbour arrangement.

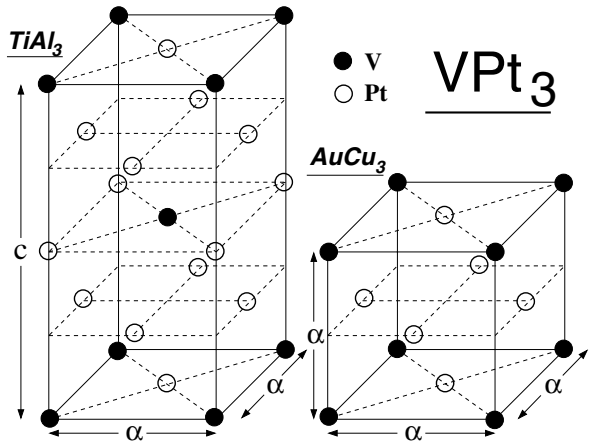

Figure 2. VPt_3 crystallizes both in the metastable cubic $AuCu_3$ structure ($L1_2$) and the tetragonal $TiAl_3$ structure (DO_{22}) which is the ground state. The c/a ratio for the $TiAl_3$ structure is 2.027, and a is slighter smaller than in the $AuCu_3$ structure. The two structures have the same type of nearest neighbour, so their relative stability is determined but the next-nearest- and further-neighbour arrangement.

To compute the magnetic properties of these compounds we used the FP-LMTO method [19] in conjunction with the Hedin–Lundquist parametrized LSDA [20]. In order to obtain well converged basis functions, a so-called double basis set was employed, with two 4s, 4p and 3d orbitals for the transition metal atom and two 6s, 6p and 5d orbitals for the gold and platinum atoms. In order to achieve convergence in the case of VAu_4 we had to treat the 3s and 3p states of vanadium and the 5p states of gold as semi-core while for the other compounds no semi-core states were needed to converge our calculations. The $\boldsymbol{k}$-space was sampled using a special-$\boldsymbol{k}$-point method and a small Gaussian of width 10 mRyd was associated with the eigenvalues close to the Fermi level, E_F, in order to speed up convergence. The MCA values of VAu_4 and $MnAu_4$ were converged within 0.01 meV with respect to the number of $\boldsymbol{k}$-points used to perform the integrations in the first Brillouin zone, i.e., 1000 $\boldsymbol{k}$-points in the full Brillouin zone were used to achieve convergence. The spin–orbit interaction was included at each variational step, a method that is known to reproduce the results from the spin-polarized Dirac equation with great accuracy [23].

3. Magneto-crystalline anisotropy

In 1980 Adachi *et al* [5] suggested that VAu_4 shows an extraordinary MCA at low temperatures because (i) the magnetization curve showed a hard saturation with a large hysteresis and (ii) the magnetic moment depended on mechanical treatment such as compression. They found that the magnetization axis is along the [001] direction and a MCA value of 0.8 meV per unit cell (u.c.) at 4.2 K. They also found that the shape anisotropy due to magnetic dipole interactions is about 0.01 meV/(u.c.) which is two orders of magnitude smaller than the MCA value. A tight-binding calculation by Yahagi *et al* yielded a MCA value of 1.0 meV/(u.c.) [1].

To our knowledge, our calculation is the first attempt to determine the MCA of the V(Mn)Au_4 compounds using an *ab initio* method. Our calculated easy-magnetization axis is the *c*-axis, [001], for both compounds, in agreement with the experiments of Adachi *et al* on VAu_4. This axis is the one with the highest symmetry; all four gold atoms are equivalent. The converged MCA value, defined as the energy difference between the [010] and the [001] axis, is 1.8 meV/(u.c.) for VAu_4, considerably larger than the experimental value, and 0.4 meV/(u.c.) for $MnAu_4$. The computation of the MCA is a difficult task and the temperature effects not taken into account in our calculations may be important. In the case of VPt_3 in the $TiAl_3$ structure we were not able to converge the value of the MCA because of the large number of inequivalent atoms in the unit cell which made this calculation too time-consuming.

4. Magnetic moments

4.1. Density of states

In the case of V(Mn)Au_4 the magnetic properties of both the 3d and gold atoms are mainly characterized by the d-type orbitals. In figures 3 and 4 we present the d-projected and spin-resolved density of states (DOS) for both atoms for the magnetization along the [001] axis. The vanadium and manganese 3d states are higher in energy than the gold states and the occupied states are mainly of spin-up character. The bandwidth of the vanadium and manganese d bands is considerably smaller than that of the gold d bands. As we add two valence electrons to the system and pass from vanadium to manganese, the spin-up states become completely occupied, their binding energy increases and they are located between −3 eV and −2 eV. This is reflected by a larger manganese spin moment compared to that of V. The spin-down states for both vanadium and manganese atoms lie 2 eV above the Fermi level and do not vary much between the different compounds. The gold 5d electrons are deeper in energy and have a bandwidth located between −9 eV and −2 eV for both compounds. The spin-up and spin-down

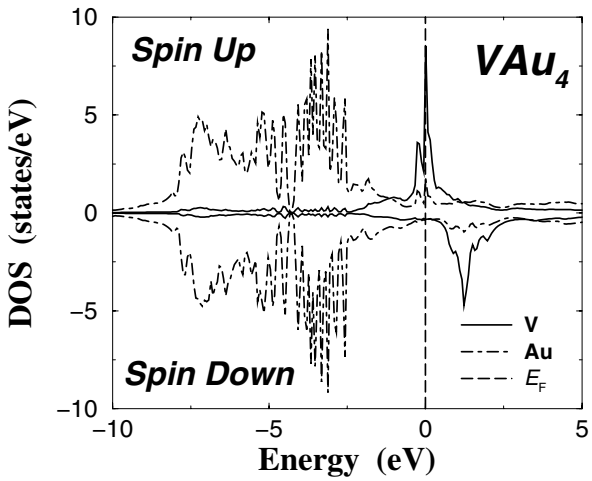

Figure 3. The relativistic d-projected density of states (DOS) for both vanadium and gold atoms in the VAu_4 system. The magnetization axis is along the [001] direction, so the four gold atoms are equivalent. Vanadium occupied states are principally of spin-up character and they are located near the Fermi level, while gold's occupied states are essentially lower in energy. The gold spin-up 5d states near the Fermi level are polarized by the vanadium spin-up 3d electrons and carry the weak gold spin magnetic moment.

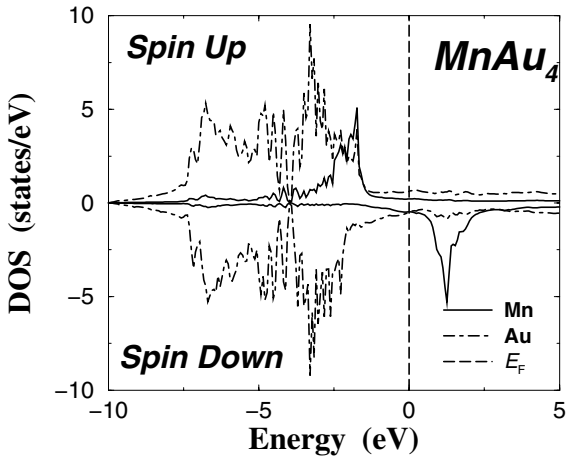

Figure 4. As figure 3, but for the $MnAu_4$ compound. The gold-atom DOS is located at the same position as for VAu_4 and has the same shape. Manganese spin-up states are deeper in energy than the V ones, and the associated bandwidth is larger. The large manganese spin moment leads to a strong hybridization with the gold spin-up d states located at −2 eV and to a larger gold spin moment compared to that of VAu_4.

DOS are similar except in the energy region where the 3d spin-up bands of the transition metal atom have their major weight. In figure 3, we can see that near the Fermi level the gold spin-up states follow the form of the vanadium spin-up states which exhibit a double-peak structure. This small polarization of the gold spin-up states by the vanadium 3d spin-up electrons is responsible for the weak gold spin magnetic moment (see table 1). A similar phenomenon occurs in the case of the $MnAu_4$ compound as can be seen in figure 4. The manganese spin-up states possess a peak located at about 2 eV below the Fermi level. At this location also the gold spin-up states have a peak and this polarization is responsible for the gold spin moment in this compound. The polarization of the gold 5d states is considerably weakened in the presence of 3d ferromagnetic atoms compared to the case for other paramagnetic elements like platinum or palladium due to the fact that the d states are practically completely occupied. But nevertheless the behaviour described above is a clear sign of hybridization between the gold and the vanadium or manganese d states.

In the case of VPt_3, the vanadium bands are wider (see figure 5). The main difference between the two possible structures of VPt_3 is related to the exchange splitting of the two d bands (the DOS is dominated by the d contributions). In the case of the $AuCu_3$ structure the Fermi level is in the middle of the spin-up band and the occupied states are mainly of spin-up character, leading to a large vanadium spin moment. But in the case of the $TiAl_3$ structure both spin-up and spin-down states are occupied and the resulting vanadium spin moment is much smaller (see table 2). The Pt states, as was the case for the gold states, follow the features of the vanadium d states in the energy region where the vanadium d states have their dominant weight. Here we should mention that our DOS for both structures are similar to those obtained by Kübler [11] although our peaks are wider and lower in intensity. Williams *et al* [24] have shown that in the case of VPd_3 the Stoner mechanism can account only for a small fraction of the magnetism because the vanadium peak in the paramagnetic case is very slightly populated. So magnetism in VPd_3 is due mainly to a redistribution of the spectral weight between the two spin-up and spin-down bands. This type of magnetism is known as covalent magnetism. Kübler showed that this is also the case for the VPt_3 compound [11].

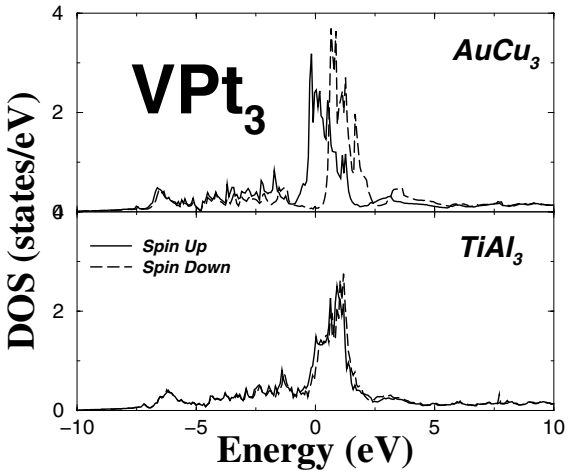

Figure 5. The vanadium spin-up- and spin-down-resolved DOS in the compound VPt_3 for both $AuCu_3$ and $TiAl_3$ structures. In the case of the first structure the exchange splitting of the two d bands is larger leading to a large vanadium spin magnetic moment compared to that of the $TiAl_3$ structure.

Table 1. Spin (μ_{spin}) and orbital (μ_{orb}) moments for both transition metal and gold atoms in VAu_4 and $MnAu_4$ compounds and for VCu_4 calculated using the same lattice parameters as for VAu_4. ** corresponds to the calculations where we have turned off the spin–orbit coupling on the gold atoms. The spin and orbital magnetic moments at the vanadium site in VAu_4 are parallel for both magnetization axes, contrary to the predictions of the third Hund's rule. When we switch off the spin coupling at the gold site both the orbital moments of vanadium and manganese atoms change sign. This is a clear indication that ligand states can influence not only the size but also the orientation of the orbital moment of a 3d atom. These results are verified by calculations for VCu_4, where copper's spin–orbit parameter is comparable to that of vanadium, that show that the vanadium orbital moment has a different sign to that for VAu_4.

	V or Mn			Au		
	μ_{spin}	$\mu_{orb}^{[001]}$	$\mu_{orb}^{[010]}$	μ_{spin}	$\mu_{orb}^{[001]}$	$\mu_{orb}^{[010]}$
VAu_4	1.67	0.16	0.06	< 0.01	-0.01	-0.01
VAu_4**	1.71	-0.10	-0.07	< 0.01	< 0.01	~ 0
VCu_4	2.08	-0.04	-0.04	0.01	~ -0	~ -0
$MnAu_4$	3.96	-0.01	-0.01	0.02	0.01	0.01
$MnAu_4$**	3.97	0.01	0.01	0.03	~ 0	~ 0

Table 2. Spin and orbital moments of the VPt_3 compound in both the $AuCu_3$ and $TiAl_3$ structures. As in table 1, the double asterisk ** denotes calculations where we have switched off the spin–orbit coupling on the Pt atoms. This causes the V orbital moment to change sign as was the case for the VAu_4 compound.

VPt_3	μ_{spin}^{V}	μ_{orb}^{V}	μ_{spin}^{Pt}	μ_{orb}^{Pt}
$AuCu_3$	1.37	0.03	-0.06	-0.03
$AuCu_3$**	1.39	-0.04	-0.06	~ 0
$TiAl_3$	0.23	0.02	-0.01	-0.01
$TiAl_3$**	0.29	-0.01	-0.01	~ 0

4.2. VAu_4 and Mn_4

The large exchange splitting of the vanadium and manganese d bands leads to a considerably enlarged localized spin moment of 1.67 μ_B for the vanadium and 3.96 μ_B for the manganese (see table 1 for the values of the magnetic moments). The gold 5d spin moments are negligible compared to the spin moments of the transition metal atoms. The larger moment of the

manganese compared to the vanadium leads to a larger polarization of the gold d bands and to a larger gold spin moment: 0.02 μ_B for $MnAu_4$ compared to 0.004 μ_B for VAu_4. Previous *ab initio* calculations by Kübler [11] and Oppeneer *et al* [12] have also found large vanadium spin magnetic moments, 1.8 and 1.78 μ_B respectively (in reference [12], the total vanadium moment of 1.90 μ_B is decomposed into a spin moment of 1.78 μ_B and an orbital contribution of 0.12 μ_B). All of these values are considerably larger than the experimental value of 1.0 μ_B [5]. It seems that the LSDA overestimates the polarization of the vanadium atoms in this material. This seems to be the case also for VPt_3 as we will discuss in the next session. For $MnAu_4$, Oppeneer *et al* [12] have found a manganese spin moment of 4.02 μ_B (the manganese orbital moment in these calculations is negligible compared to the spin moment) which is very close to our results of 3.96 μ_B. Both calculations agree well with the experimental value of 4.0 μ_B [10].

The spin magnetic moments vary with the magnetization axis only for the vanadium atom in VAu_4, but this variation is small: 1.67 μ_B for the easy-magnetization axis, [001], and 1.71 μ_B for the hard-magnetization axis, [010]. This small change in the spin magnetic moment is accompanied by a considerable change in the DOS as can be seen in figure 6. For the [001] axis the DOS near the Fermi level presents a two-peak structure with a very intense second peak just above the Fermi level. For the hard axis these peaks become less intense. The DOS of the gold atoms does not display any change in going from one magnetization axis to another.

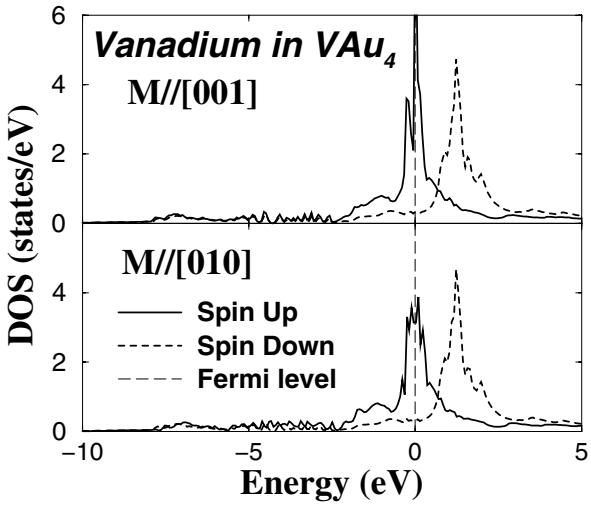

Figure 6. The calculated d-projected density of states of the vanadium atom for two magnetization directions in VAu_4. The spin-up band for the easy [001] axis shows a sharp peak, which is not present for the hard [010] axis. The two d spin-up bands have the same bandwidth. The spin-down bands are practically the same for the two magnetization axes.

The most interesting feature of both VAu_4 and $MnAu_4$ compounds is the orbital magnetic moments that are presented in table 1. First we remark that the vanadium atoms do not obey Hund's third rule. For vanadium, spin and orbital magnetic moments are parallel while for manganese they are anti-parallel. We will discuss this behaviour in the next section of our paper. The vanadium orbital moments are one order of magnitude larger than the manganese orbital moments and present a large anisotropy: 0.16 μ_B for the [001] axis and 0.06 μ_B for the [010] axis. This large orbital moment anisotropy can explain the large Kerr effect anisotropy predicted for this material [12].

To explain the large vanadium orbital moment anisotropy we projected the d DOS on the m_ℓ basis. To calculate the orbital magnetic moment $\mu^{\ell}_{q,orb}$ of the atom q, we use the expression

$$\mu^{\ell}_{q,orb} = \sum_{\sigma}\sum_{m_\ell} m_\ell \int_{-\infty}^{E_F} D^{q}_{\ell,m_\ell,\sigma}(E)\,\mathrm{d}E \tag{1}$$

where $D^{q}_{\ell,m_\ell,\sigma}(E)$ is the projected density of states on each muffin-tin sphere q and on the ℓ, m_ℓ, σ basis (where ℓ, m_ℓ are the angular momentum quantum numbers and σ the electron spin). The integral is taken up to the Fermi level E_F. In figure 7 we show the spin-up d states of V projected on $m_\ell = \pm 1$ for both magnetization axes. We see that for both axes the contribution to the vanadium orbital magnetic moment is positive and the absolute value for the easy axis is considerably larger. The $m_\ell = \pm 2$ states show a similar behaviour as can be seen in figure 8. In table 3 we have collected the values for the contributions of each m_ℓ d-projected state to the orbital moment for the spin-up states, which is, as derived from equation (1),

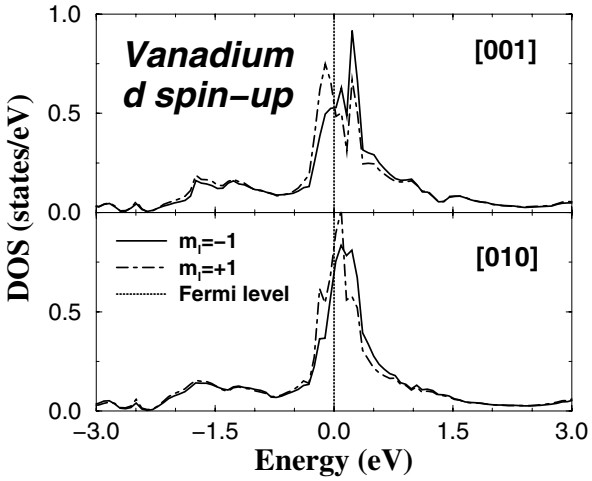

Figure 7. The calculated d-projected spin-up density of states of the vanadium atom projected on the $m_\ell = \pm 1$ quantum numbers for VAu_4. We remark that for the easy axis [001] the total contribution to the orbital magnetic moment is positive and its absolute value is larger than for the hard axis [010].

Table 3. Contributions of each m_ℓ-projected density of states to the vanadium spin-up d orbital magnetic moment in VAu_4 for both magnetization axes. The states with $m_\ell = \pm 2$ make a more important contribution to the orbital moment than the states with $m_\ell = \pm 1$, but for the hard axis, [010], the two contributions are practically equal. The spin-up-resolved contributions dominate the orbital moment. Finally notice that there are mainly states with positive m_ℓ for the easy axis that move towards states with $m_\ell = 0$ for the hard axis that are responsible for the orbital moment anisotropy.

μ^{V}_{orb}(spin-up)	[001]	[010]
$m_\ell = -2$	−1.065	−1.063
$m_\ell = -1$	−0.463	−0.453
$m_\ell = +1$	0.518	0.488
$m_\ell = +2$	1.153	1.101
$m_\ell = \pm 1$	0.055	0.035
$m_\ell = \pm 2$	0.088	0.038
Total	0.143	0.073

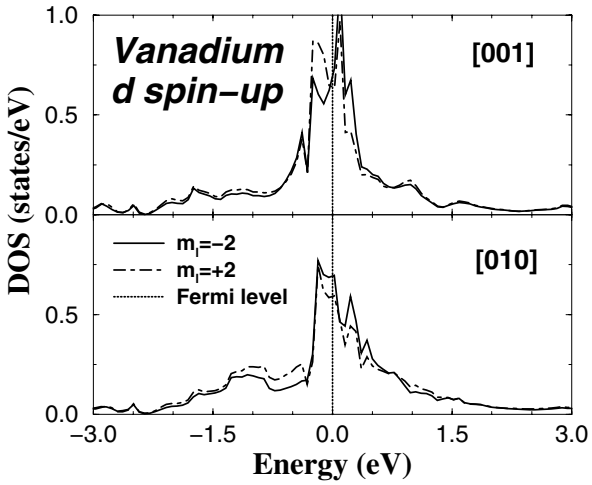

Figure 8. The calculated d-projected spin-up density of states of the vanadium atom projected on the $m_\ell = \pm 2$ quantum numbers for VAu_4. As for the $m_\ell = \pm 1$ case (see figure 7) the total contribution to the orbital magnetic moment is larger for the easy axis [001].

nothing more than the integral of the equivalent DOS over the occupied states multiplied by the value of the m_ℓ. We notice that the spin-up total orbital magnetic moments are slightly different from the total ones in table 1 suggesting that the spin-down states contribute little to the orbital anisotropy and hence we do not show them. The numbers in this table reflect the above discussion. The states with $m_\ell = \pm 2$ contribute 0.088 μ_B to the orbital magnetic moment for the easy axis and just 0.038 μ_B for the hard one, whereas the states with $m_\ell = \pm 1$ contribute 0.055 μ_B to the orbital magnetic moment for the easy axis and 0.035 μ_B for the hard one. Finally, it is interesting to notice that the partial DOS in the region just below the Fermi level shows a change of states with character $m_\ell = 1$ and $m_\ell = 2$ for the easy axis to states with $m_\ell = 0$ for the hard axis, explaining the origin of the large orbital magnetic moment anisotropy. The states with $m_\ell = 0$ make zero contribution to the orbital moment. The number of states with $m_\ell = -2$ is practically the same for the two magnetization directions, while the change in the number of states with $m_\ell = -1$ is less important than that for the states with positive values of m_ℓ.

4.3. VPt_3

In table 2 we have gathered the spin and orbital moments of both vanadium and Pt atoms for both possible crystallographic structures. In the case of the $AuCu_3$ structure the magnetization axis was considered to be [111] and for the $TiAl_3$ structure [001]. Actually, in the case of the $AuCu_3$ structure we calculated the magnetic moments also for the [001] and [110] axis and, except for the Pt orbital moment which shows small changes between the different axes, all the other values were found to be practically insensitive to the magnetization axis. As was found in previous calculations [2, 16–18], vanadium in the $AuCu_3$ structure has a large spin magnetic moment of 1.37 μ_B, considerably larger than the value of 0.23 μ_B in the case of the $TiAl_3$ ground-state structure. VPt_3 in the $TiAl_3$ structure was first studied by Kübler [11] who found it to be practically a paramagnet. However, in his calculations he did not take into account the spin–orbit coupling that should enhance the tendency towards ferromagnetism, due to stronger orbital contributions. This hypothesis was verified by Auluck and Nautiyal

who found for the vanadium a spin magnetic moment of 0.41 μ_B [18], larger than our value of 0.23 μ_B. For both structures we see that the vanadium spin and orbital moments are parallel as was the case for VAu_4, although here the absolute values of the orbital moments are smaller than in the case of VAu_4. The V orbital moment has been previously calculated only for the $AuCu_3$ structure by Oppeneer *et al* [17] who have found a value of 0.02 μ_B close to our value of 0.03 μ_B. Due to the larger vanadium spin moment in the $AuCu_3$ structure, the induced Pt spin moment for this structure is much larger than for the $TiAl_3$ structure: $-0.06\ \mu_B$ compared to $-0.01\ \mu_B$. This difference in the spin moments is also reflected in the orbital moments which are quite large compared to the spin moments due to the large spin–orbit coupling of Pt. Both our spin and orbital Pt moments for the $AuCu_3$ structure agree with previous *ab initio* calculations [11, 16, 17]. We are not aware of any calculation prior to ours for the Pt magnetic moments in the $TiAl_3$ structure of VPt_3.

Experimentally, Jesser *et al* have measured the total spin moment per unit cell and found a value of 0.1 μ_B for both structures [14]. In the case of $TiAl_3$ structure the total calculated spin moment is 0.20 μ_B, i.e. twice the experimental one, but of the same order, while in the case of the $AuCu_3$ structure the total calculated spin moment per unit cell is 1.19 μ_B which is one order of magnitude larger than the experimental value of Jesser *et al*. To explain the latter discrepancy we should refer to the experimental work of Kawakami and Goto [15]. They estimated in the case of the $AuCu_3$ structure a vanadium spin magnetic moment of 1 μ_B and a Pt spin magnetic moment of 0.3 μ_B [15], the latter being one order of magnitude larger than all of the calculated values; our value is $-0.06\ \mu_B$ and previous calculations found a value of $-0.05\ \mu_B$ [11, 17]. Using these experimental values, the total spin moment per unit cell is $\mu_{spin}^{total} = \mu_{spin}^{V} + 3\mu_{spin}^{Pt} = 1.0\ \mu_B + 3(-0.3)\ \mu_B = 0.1\ \mu_B$ in agreement with the experiments of Jesser *et al*. So the large discrepancy in the case of the $AuCu_3$ structure comes from the strong underestimation of the Pt spin moment by our theory compared to experiments. In the case of other compounds like FePt, CoPt or $CoPt_3$ where the Pt spin moment is also about 0.2–0.3 μ_B, the calculated values agree nicely with experiments [25]. It seems that the LSDA fails to describe well the hybridization in the case of ferromagnetic materials that consist of two elements that are paramagnetic in their bulk form, but no explanation of this phenomenon is available. We could just speculate that it could be that it is difficult to experimentally achieve full magnetic saturation, or that the spin fluctuations, not taken into account in the LSDA, are large in this particular case.

5. Tuning the transition metal orbital moment

As already mentioned in the previous sections, the vanadium orbital moment for both VPt_3 and VAu_4 compounds does not obey the third Hund's rule that states that for vanadium the spin and orbital moments should be anti-parallel since the filling of the d shell is less than half-filled. Although Hund's rules were derived originally for atoms, the comprehension of the origin of their violation in a transition metal alloy, like the ones studied here, is important because it may lead to an understanding of how to tune the orbital moment of a 3d atom in a magnetically ordered material. The only possible source for the reversal of vanadium's orbital moment is the influence of the ligand states on the magnetic properties of the 3d atom. It has been already shown, using a first-order perturbation theory both in the direct [26] and in the reciprocal space [27], that the spin–orbit coupling of the ligand atom contributes to the orbital moment of the 3d atom. In the case of the binary compounds Fe(Co)–Pd(Pt) studied by Solovyev *et al*, this contribution affected the size of the iron(cobalt) orbital moment but was not strong enough to change its sign [26]. But this becomes possible in the case of VPt_3 and VAu_4 due to the large spin–orbit coupling parameter for both Pt and Au.

In order to test this further we performed calculations of the spin and orbital moments of VAu_4 and VPt_3, turning off the spin–orbit interaction at the gold and platinum sites, but keeping it for the vanadium site. We also performed calculations for the VCu_4 compound using the lattice constants of the VAu_4, since the strength of the spin–orbit coupling parameter of copper is comparable to that of vanadium and much smaller than that of Au. We have collected our results in tables 1 and 2. In all of these cases the spin and orbital moments at the vanadium site are anti-parallel. The calculated spin and orbital moments of the vanadium atom in VAu_4, where we have switched off the spin–orbit coupling on the gold atoms, are 1.71 μ_B and -0.10 μ_B, respectively. In the case of VCu_4 the spin and orbital moments are 2.08 μ_B and -0.04 μ_B respectively. For VPt_3 the vanadium orbital moment is smaller than in the case of VAu_4 but switching off the Pt spin–orbit coupling obliges the vanadium orbital moment to change sign for both structures following the same behaviour as VAu_4. Finally, we performed a calculation for $MnAu_4$ without the spin–orbit coupling at the gold site (see table 1) and we observe that the manganese orbital moment also changes sign. These values demonstrate that the large spin–orbit couplings of the gold and platinum atoms influence, via hybridization, the orbital moment of the neighbouring transition metal atom to a surprisingly large extent, reversing the direction of the transition metal orbital moment.

A very interesting scenario now emerges, since by suitable tuning of copper and gold concentrations one may fabricate an alloy of $V(Au_xCu_{1-x})_4$ that has a vanishingly small orbital moment on the vanadium atom. The orbital magnetic moment, although it is small in some of the pertinent materials, nevertheless has been argued to carry vital information about the MCA [28]. As a matter of fact, using perturbation theory, the directional dependence of the orbital moment has been shown to be proportional to the MCA by Bruno [29] and this finding, although it has been argued not always to hold, must be considered as being important in establishing a microscopical understanding of the MCA of delocalized electron systems. In the case of VAu_4, Bruno's relation is expected to hold because the occupied states are practically all of spin-up character. To study the relation between calculated orbital moment and calculated MCA, we calculated the vanadium orbital moment for the easy axis and the MCA for an alloy of $V(Au_xCu_{1-x})_4$ for all integer values of x and assuming the lattice parameters of VAu_4. We present our results in table 4. The vanadium orbital moment for the hard axis ([010]) is zero for all of the compounds except VAu_4. Substituting copper for gold causes the vanadium orbital moment to decrease and the calculated MCA decreases also. In the case of VAu_2Cu_2 where the gold and copper atoms are positioned symmetrically with respect

Table 4. Vanadium spin and orbital moments for VAu_xCu_{4-x} compounds and for the easy [001] axis. For the [010] axis, vanadium's orbital moment is zero for all materials except VAu_4. The partial substitution of copper for gold leads to a considerable decrease of the vanadium orbital moment and of the calculated MCA. In parenthesis the experimental MCA value from reference [5] is given. For the VAu_2Cu_2 compound there exist two different ways to arrange the two gold and the two copper atoms. The first way, denoted by (1), is that where the gold atoms occupy the positions 1 and 2 (see figure 1) and the second, denoted by (2), that where they are symmetric with respect to the vanadium atom and thus they occupy the positions 1 and 3. The substitution of copper atoms for gold ones decreases the vanadium orbital moment and changes the calculated MCA.

	μ^{V}_{spin}	μ^{V}_{orb}	MCA (meV)
VAu_4	1.67	0.16	1.8 (0.8)
VAu_3Cu	1.73	0.07	1.1
VAu_2Cu_2 (1)	1.82	0.04	0.9
VAu_2Cu_2 (2)	1.86	0.03	0.5
$VAuCu_3$	1.94	~ -0	0.6

to the vanadium atom, the vanadium orbital moment is 0.03 μ_B, less than one fifth of the value for VAu_4 (the orbital moment anisotropy is one third), and the MCA for this compound is only 0.5 meV, practically one fourth of the value for VAu_4. For $VAuCu_3$ the vanadium orbital moment changes sign, although it is very close to zero and the MCA becomes slightly larger than for VAu_2Cu_2. One may observe that the non-cubic system studied here, $V(Au_xCu_{1-x})_4$, may not be ideal in this regard, since cubic materials are known to have much smaller influence of the spin–orbit coupling, and hence lower values of the MCA. Nevertheless, the procedure presented here for manipulating the orbital moment and MCA should be useful in the search for ultra-soft magnets.

6. Conclusions

To summarize, we have studied the magnetic properties of the VAu_4, $MnAu_4$ and VPt_3 compounds. First, we calculated the magneto-crystalline anisotropy and verified that the easy magnetization axis is [001] for both VAu_4 and $MnAu_4$. Our calculations overestimate the polarization of the vanadium d orbitals, producing a larger vanadium spin magnetic moment than the one obtained experimentally, while the manganese calculated spin moment agreed nicely with experiment. We have explained the vanadium orbital moment anisotropy in VAu_4 as arising from a change of states characterized by a positive m_ℓ for the easy [001] axis towards an $m_\ell = 0$ character for the hard [010] axis.

We have shown that the gold and Pt spin–orbit coupling is responsible for the reversal of vanadium and manganese orbital magnetic moment in these compounds. The possibility of tuning the orbital moment and the MCA by suitable alloying has been proposed for $V(Au_xCu_{1-x})_4$ compounds, which may open up a new avenue in the search for ultra-soft magnetic materials.

Acknowledgments

The support from the TMR of 'Interface Magnetism' and the Swedish Foundation for Strategic Research (SSF) are acknowledged. OE is grateful to NFR and TFR for support. We are grateful to Dr J M Wills for providing the full-potential code used in this work. Valuable discussions and the support from Professor B Johansson are acknowledged. IG is supported by a fellowship from the EU (grant ERBFMXCT96-0089).

References

[1] Yahagi H, Yano K, Itoga H, Chaki A, Ukai T and Mori N 1991 *J. Appl. Phys.* **69** 4651
[2] Tohyama T, Ohta Y and Shimizu M 1989 *J. Phys.: Condens. Matter* **1** 1789
[3] Creveling L, Luo H L and Knapp G S 1967 *Phys. Rev. Lett.* **18** 851
[4] Creveling L and Luo H L 1968 *Phys. Rev.* **176** 614
[5] Adachi K, Matsui M and Fukuda Y 1980 *J. Phys. Soc. Japan* **48** 62
[6] Kido G, Miura N, Matsui M and Adachi K 1983 *J. Magn. Magn. Mater.* **31–34** 283
[7] Chin G Y, Sherwood R C, Wernick J H, Mendorf D R and Knapp G S 1968 *Phys. Lett.* A **27** 302
[8] Sill L R, Kimball C W, Clark R H, Mass W J and Darby J B 1970 *J. Appl. Phys.* **41** 865
[9] Claus H, Sinha A K and Beck P A 1967 *Phys. Lett.* A **26** 38
[10] Yessik M, Noakes J and Sato H 1971 *J. Appl. Phys.* **42** 1349
[11] Kübler J 1984 *J. Magn. Magn. Mater.* **45** 415
[12] Oppeneer P M, Galanakis I, James P, Eriksson O and Ravindran P 1999 *J. Magn. Soc. Japan* **23** 21
[13] Turek P, Kuentzler R, Bieber A and Jesser R 1985 *Solid State Commun.* **53** 979
[14] Jesser R, Bieber A and Kuentzler R 1981 *J. Physique* **42** 1157
[15] Kawakami M and Goto T 1979 *J. Phys. Soc. Japan* **46** 1492

[16] Iwashita K, Oguchi T and Jo T 1996 *Phys. Rev.* B **54** 1159
[17] Oppeneer P M, Antonov V N, Kraft T, Eschrig H, Yaresko A N and Perlov A Ya 1996 *J. Phys.: Condens. Matter* **8** 5769
[18] Auluck S and Nautiyal T 1989 *Phys. Rev.* B **39** 8718
[19] Wills J M and Cooper B R 1987 *Phys. Rev.* B **36** 3809
Alouani M and Wills J M 1996 *Phys. Rev.* B **54** 2480
Wills J M, Eriksson O, Alouani M and Price D L 2000 *Electronic Structure and Physical Properties of Solids: the Uses of the LMTO Method (Springer Lecture Notes on Physics vol 535)* ed H Dreyssé (Berlin: Springer)
[20] Hedin L and Lundquist S 1971 *J. Phys. C: Solid State Phys.* **4** 2064
[21] von Barth U and Hedin L 1972 *J. Phys. C: Solid State Phys.* **5** 1629
[22] Dwight A E, Downey J W and Conner R A 1961 *Acta Crystallogr.* **14** 75
[23] Compare for instance the orbital moments of the two methods in
Söderlind P *et al* 1995 *Phys. Rev.* B **45** 12 911
Strange P, Ebert H, Staunton J B and Györffy B L 1989 *J. Phys.: Condens. Matter* **1** 3947
and see also
Strange P, Staunton J B, Györffy B L and Ebert H 1991 *Physica* B **172** 51
[24] Williams A R, Zeller R, Moruzzi, Gelatt C D and Kübler J 1981 *J. Appl. Phys.* **52** 2067
[25] Galanakis I, Alouani M and Dreyssé H 2000 *Phys. Rev.* B **62** 6475
[26] Solovyev I V, Dederichs P H and Mertig I 1995 *Phys. Rev.* B **52** 13 419
[27] Galanakis I, Oppeneer P M, Ravindran P, Nordström L, James P, Alouani M, Dreyssé H and Eriksson O 2001 *Phys. Rev.* B **63** 172405
[28] Weller D, Wu Y, Stöhr J, Samant G, Hermsmeier B D and Chappert C 1994 *Phys. Rev.* B **49** 12 888
[29] Bruno P 1989 *Phys. Rev.* B **39** 865